

Matrix-Isolation FT-IR Studies and Theoretical Calculations of Different Types of Hydrogen-Bonding: 2-Hydroxypyridine/2-Oxopyridine Complexed with HCl

A. Dkhissi,[†] L. Houben,[†] R. Ramaekers,[†] L. Adamowicz,[‡] and G. Maes^{*,†}

Department of Chemistry, University of Leuven, Celestijnenlaan 200F, B3001 Heverlee, Belgium, and Department of Chemistry, University of Arizona, Tucson, Arizona 85721

Received: May 24, 1999; In Final Form: September 17, 1999

The H-bond interaction of the cytosine model compound 2-hydroxypyridine and its tautomer 2-oxopyridine with HCl is investigated using the combined matrix-isolation FT-IR and theoretical density functional and ab initio methods. The theoretical calculations have been carried out at the B3-LYP/6-31++G** and RHF/6-31++G** levels of theory. Different types of hydrogen-bonding have been found: two closed complexes of the proton transfer type, each containing two hydrogen bonds, i.e., $N^+-H\cdots Cl^- \cdots H-O$ and $C=O^+-H\cdots Cl^- \cdots H-N$; two open complexes of intermediate strength, $N\cdots H-Cl$ and $C=O\cdots H-Cl$; and one weak complex, $H-O\cdots H-Cl$. The theoretical results indicate that the closed H-bonded complexes are the most stable systems for both the hydroxy and the oxo tautomers. The increased stability of these complexes is due to a cooperative H-bonding effect. The experimental spectra are consistent with this prediction, but the weaker complexes are also identified. A comparison of the experimental and calculated IR frequencies demonstrates that the frequency shifts of the vibrational modes directly involved in the H-bond interactions, especially the X–H stretching modes, are better predicted by the DFT method than by the RHF method. For the other vibrational modes not directly involved in the H-bonds, the RHF methodology has a similar accuracy compared to the DFT method.

1. Introduction

The hydrogen halides HF and HCl have been widely used in experimental studies of H-bonded complexes isolated in low-temperature inert matrices.^{1–5} Large series of complexes with bases varying from extremely weak (e.g., N₂ with a proton affinity (PA) value of 503 kJ·mol⁻¹) to very strong (e.g., trimethylaminoxide with PA 999 kJ·mol⁻¹).⁶ The so-called correlation diagram⁷ relates the relative frequency shift $\Delta\nu(X-H)/\nu^\circ(X-H)$ of the H–X mode ν_s with the normalized PA difference between the base and the anion X⁻, which has allowed a classification of H-bonds into different types: type I or “normal” H-bonds B \cdots H–X characterized by $\Delta\nu_s/\nu_s^\circ$ values of less than 20%; type II or “symmetrical” H-bonds B \cdots H \cdots X with a more or less perfect proton sharing between X⁻ and B, with $A\nu_s/\nu_s^\circ$ values as large as 80%; and finally type III or “proton-transfer” H-bonds B–H⁺ \cdots X⁻ corresponding to an ion pair where the proton donor mode ν_s is replaced by the ν_{BH^+} mode of the proton-transfer species. Type I H-bonds are weak or moderate hydrogen bonds, while types II and III are strong hydrogen bonds. Type II H-bonds are formed when the proton is shared by two strong bases such as in the [F–H–F]⁻ ion. It should be mentioned that these strong hydrogen bonds play an important role in enzyme catalysis,⁸ whereas the proton-transfer process is of huge importance in biology⁹ and zeolite chemistry.^{10,11} For example, the spectral identification of the ion pair and neutral hydrogen bonds involving pyridine is important for the elucidation of the mechanisms of zeolite catalysis.¹⁰

In our formerly published results for complexes of different bases with HCl in Ar matrices,^{12–14} the complexes appeared to be of type II and intermediate type I \rightarrow II. Furthermore, it was

observed that these systems give rise to proton transfer at higher HCl concentration or after the matrix samples are annealed.

In the series of continuing experimental and theoretical investigations of tautomeric and H-bonding properties (with H₂O) of nucleic acid bases and some model molecules,^{15–23} we have also studied the H-bond interaction of the prototropic compound 2-hydroxypyridine (hydroxy \leftrightarrow oxo, denoted as 2HP \leftrightarrow 2OP)^{24–26} (theoretical PA 915 and 898 kJ·mol⁻¹, respectively),²⁷ with HCl in Ar matrices. Our interest in these complexes originates from the latter PA values which suggest that different types or intermediate types of complexes might occur.

Because we have demonstrated in earlier reports^{15–23} that coupling of matrix-isolation FT-IR spectrometry to ab initio computational methods is one of the most suitable approaches for evaluating intrinsic tautomeric and H-bonding characteristics of polyfunctional bases, we have applied the same approach to the hydrogen-bonding between the tautomers 2HP/2OP and HCl. However, in a further stage we have compared the results of the DFT/B3-LYP/6-31++G** study with those obtained from the RHF/6-31++G** method and with the matrix FT-IR experimental results. Five different complexes have been identified from the FT-IR spectra supported by the theoretical calculations: two closed complexes of type III, $N^+-H\cdots Cl^- \cdots H-O$ and $C=O^+-H\cdots Cl^- \cdots H-N$; two open complexes of intermediate type I \rightarrow II, $N\cdots H-Cl$ and $C=O\cdots H-Cl$; and finally one weak complex of type I, $H-O\cdots H-Cl$. The optimized geometries of these five complexes are shown in Chart 1.

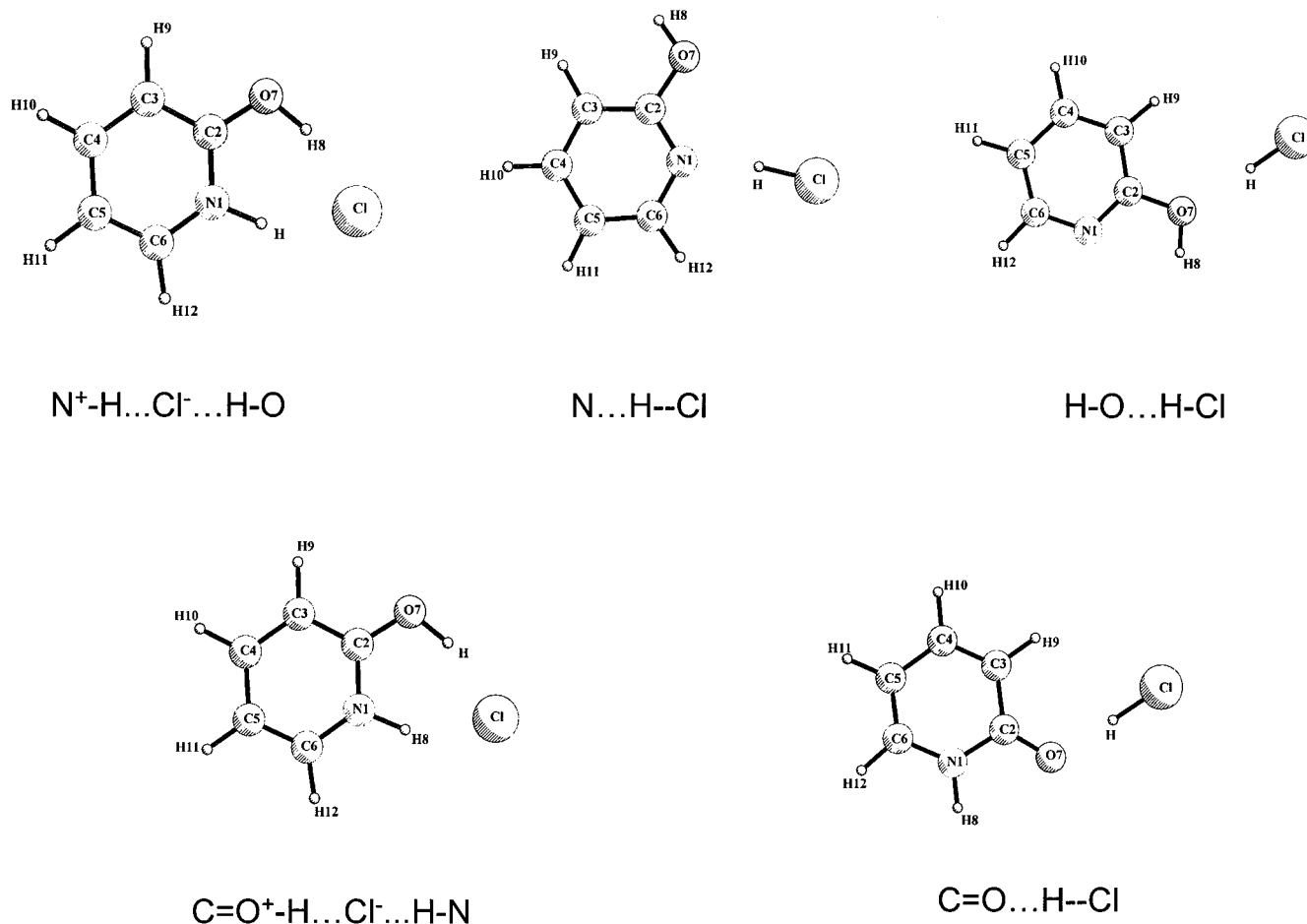
2. Methodology

2.1. Experimental Method. The solid compound 2HP (97%) was purchased from ACROS, while the employed gases Ar

[†] University of Leuven.

[‡] University of Arizona.

CHART 1: Five Possible H-Bonded Complexes of HCl with 2HP/2OP Considered in This Work



(99.9999%) and HCl (99.5%) were obtained from UCAR. The FT-IR instrument (Bruker IFS 88) and the low-temperature matrix-isolation equipment have been described in previous papers.^{28–29} The optimal temperature for sublimation of 2HP under ideal conditions in the minifurnace, installed in the cryostat, is 288 K. The HCl/Ar ratio was varied between 1/200 and 1/100, and during the annealing experiments the temperature of the matrix was raised to 35–39 K for 5–10 min.

2.2. Theoretical Method. In our recent study of the model H-bonded complex pyridine–water, we have compared the predictive abilities of different density functional methods in reproducing the experimental matrix IR results.³⁰ The purpose of that investigation was to select the most effective functional for future DFT studies on H-bonded complexes of nucleic acid bases. As expected, the study demonstrated that the shift of the OH stretching frequency of the proton donor molecule is much better predicted with the B3-LYP functional^{31,32} when diffuse functions are added to the basis set. Therefore, the latter functional is selected for this study of 2-hydroxypyridine/2-oxopyridine complexed with HCl. To compare the DFT calculations with *ab initio* methods, the RHF method was also used in the present study.

For the molecular orbital expansion we have used the 6-31++G** basis set. The choice of this basis set is based on the consideration that to obtain reliable properties for hydrogen-bonded systems, it is essential to employ basis sets that possess sufficient diffuseness and angular flexibility.³³ This basis set is sufficient to predict reliable vibrational properties for hydrogen-bonded systems, as was demonstrated in ref 30.

The computed total energy for each system includes the zero-

point vibrational energy calculated by the DFT method with a single scaling factor of 0.970. The IR frequencies and intensities were computed at the RHF and DFT levels of theory using analytical derivative procedures implemented in the Gaussian 94 program.³⁴

Finally, potential energy distributions (PEDs) are calculated and the predicted IR frequencies are scaled to account for various systematic errors in the theoretical approach. Two scaling procedures are applied: either all frequencies are scaled with a uniform scaling factor 0.900 (RHF), or scaling is performed with a set of different scaling factors (reflecting the difference in anharmonicity) depending on the different types of vibrational modes (DFT), i.e., 0.950 for $\nu(XH)$, 0.980 for the out-of-plane modes, and 0.975 for all other modes. The use of different scaling factors for frequencies belonging to different types of vibrational modes seems immanent in this case, and it has already been proposed by several other authors.^{35–38} The mechanical anharmonicity of the ν_{HCl} stretching mode of the complexes as well as of the free molecule has been calculated by the variational method.^{39,40}

3. Results and Discussion

3.1. Energetic and Structural Properties. Five equilibrium structures have been found on the 2HP/2OP–HCl energy surface (Chart 1). The calculated interaction energies and binding enthalpies at 0 K are listed in Table 1. The interaction energies calculated using B3-LYP/6-31++G** are -60.1 and -58.2 $\text{kJ}\cdot\text{mol}^{-1}$ for the $N^+-H\dots Cl^- \dots H-O$ and $C=O^+-H\dots Cl^- \dots H-N$ complexes, respectively. These values manifest

TABLE 1: Total Energies (au), Interaction Energies (kJ·mol⁻¹), Binding Enthalpies (kJ·mol⁻¹), and Dipole Moments (D) Calculated Using B3-LYP/6-31++G for Complexes of 2-Hydroxypyridine and 2-Oxopyridine with HCl**

	2-hydroxypyridine complexes			2-oxopyridine complexes	
	N ⁺ -H···Cl ⁻ ···H-O	N···H- -Cl	H-O···H-Cl	CO ⁺ -H···Cl ⁻ ···H-N	C=O···H- -Cl
<i>E</i>	-784.3699629	-784.3529671	-784.3544700	-784.3699622	-784.3630504
ZPE	0.1020139	0.0990322	0.0989885	0.1020023	0.0997946
<i>E_T</i>	-784.2679490	-784.2539350	-784.2554815	-784.2679599	-784.2632558
interaction energy	-60.1	-38.9	-19.4	-58.2	-40.1
ΔZPE ^a	13.1	6.2	5.0	12.5	6.7
Binding enthalpy at 0 K	-47.0	-32.7	-14.4	-45.7	-33.4
μ (D)	9.70	7.47	3.56	9.69	8.27

^a ΔZPE = ZPE(complex) - [ZPE(HCl) + ZPE(hydroxy/oxo)].

TABLE 2: Selected Structural Properties (Å) for Complexes of 2-Hydroxypyridine/2-Oxopyridine with HCl

		N ⁺ -H···Cl ⁻ ···H-O	H-O···H-Cl	N···H- -Cl	C=O ⁺ -H···Cl ⁻ ···H-N	C=O···H- -Cl
		<i>R</i> (N-Cl) or <i>R</i> (O-Cl) ^a	DFT	2.94	3.23	3.06
	RHF	3.00	3.38	3.32	3.00	3.19
<i>r</i> _{HCl}	DFT	1.958 (0.677)	1.301 (0.020)	1.346 (0.065)	1.887 (0.606)	1.339 (0.058)
	RHF	2.047 (0.781)	1.273 (0.007)	1.285 (0.019)	2.067 (0.801)	1.284 (0.018)
<i>r</i> _{CO}	DFT	1.305 (-0.051)	1.368 (0.01)	1.355 (-0.002)	1.305 (0.073)	1.284 (0.016)
	RHF	1.288 (-0.047)	1.344 (0.009)	1.336 (0.001)	1.288 (0.082)	1.215 (0.009)
<i>r</i> _{OH}	DFT	1.040 (0.069)	0.971 (0.000)	0.967 (-0.004)		
	RHF	0.980 (0.033)	0.948 (0.001)	0.943 (-0.004)		
<i>r</i> _{NH}	DFT			1.068 (0.055)	1.014 (0.001)	
	RHF			1.031 (0.031)	0.997 (-0.003)	

^a *R*(N-Cl) or *R*(O-Cl) represent the intermolecular distances between N and Cl and between O and Cl.

the presence of strong H-bonding in both complexes. The calculation of binding enthalpies is interesting since it often allows a direct comparison with experimental values. The binding enthalpies at 0 K of the N⁺-H···Cl⁻···H-O and C=O⁺-H···Cl⁻···H-N complexes are -47.0 and -45.7 kJ·mol⁻¹. These values are larger than those for the corresponding H-bonded complexes containing only a single H-bond N···H- -Cl (-32.7 kJ·mol⁻¹) or C=O···H- -Cl (-33.4 kJ·mol⁻¹). Last, a much weaker complex is the open H-O···H-Cl system (-14.4 kJ·mol⁻¹). The difference in the binding enthalpy of singly and doubly H-bonded complexes indicates that H-bond cooperativity occurs between the two H-bonds in the closed complexes. This effect has also been observed for pyridone-H₂O,⁴¹ 2-hydroxypyrimidine-H₂O,²² and 2-hydroxypyridine-H₂O.⁴² The interaction energy values obtained here suggest that all five complexes are stable enough to be identified from the matrix FT-IR spectra. As is also shown in Table 1, the dipole moment values increase parallel to the binding enthalpy values of the complexes.

In Table 2 we have collected selected structural properties for the five complexes calculated with DFT and RHF methods. First of all, the DFT/B3-LYP calculated intermolecular distances *R*(N-Cl) or *R*(O-Cl) are, for each system, shorter than those obtained at the RHF level. The difference between these two prediction levels must be attributed to correlation effects, which are effectively accounted for only by the DFT method. However, the dispersion energy is not included in the DFT method, and the intermolecular distance is related to this part of the energy. If one takes this energy into account, this distance will decrease. One of the most interesting structural quantities is the prolongation of the X-H bond, since this elongation is the key for a reliable interpretation (X-H frequency shifts) in the infrared vibrational spectra of the hydrogen-bonded complexes. The prolongation of the X-H bond in each complex, calculated with RHF (underlined in Table 2 for the complexes under consideration), is considerably smaller than the value obtained with the DFT/B3-LYP functional. This result suggests that the ν_{X-H} frequency shift calculated with RHF would be smaller than that obtained with the DFT method.

Chart 1 demonstrates that proton transfer occurs from H-Cl to the 2-hydroxypyridine and 2-oxopyridine, resulting in a 2-hydroxypyridinium chloride complex, N⁺-H···Cl⁻···H-O, and a 2-oxopyridinium chloride complex, C=O⁺-H···Cl⁻···H-N. For the first complex, DFT predicts a bond length *r*_{N⁺-H} of 1.07 Å (not included in Table 2), which is very close to the bond length in the phenoxy-imidazolium complex (*r*_{N⁺-H} = 1.06 Å).⁴³ For these complexes, the increase of the OH and NH distances is very large, while large dipole moments are also predicted for these strong complexes. The former effect obviously results from the presence of the two H-bonds in a closed H-bonded structure.

3.2. Experimental Results. 2-Hydroxypyridine occurs as a tautomeric mixture hydroxy/oxo in Ar matrices, with a tautomerization constant *K_T*(oxo/hydroxy) varying from 0.36 to 0.46.^{24,26} As a matter of fact, the IR spectrum of the matrix-isolated compound is rather complicated as it exhibits intense ν_{OH}, ν_{NH}, and ν_{C=O} absorptions, as well as a very rich fingerprint pattern.^{24,26} A further complication with this compound is that the vicinal position of the two H-bonding sensitive groups, OH and N for the hydroxy form and C=O and NH for the oxo form, allows the formation of closed H-bonded structures with HCl. For the experimental analysis, three regions of the IR spectra of 2HP ↔ 2OP/Ar/HCl are selected. In the region 1800-400 cm⁻¹ illustrated in Figure 1, two new IR absorptions are observed at 1620 cm⁻¹ (very broad and superimposed upon the ν(C=O) Fermi pattern) and 1400 cm⁻¹ (more or less broad). These bands can be interpreted as the shifted HCl stretching modes in the C=O···H- -Cl and N···H- -Cl complexes, respectively. The location of these typical ν_s bands suggests H-bonds of the intermediate I → II type, which is similar to the results earlier obtained for the uracil/HCl/Ar system.^{12,13} A further argument in favor of this assignment is the proton affinity value of the 2OP tautomer (898 kJ·mol⁻¹), which is close to the proton affinity of uracil (870 kJ·mol⁻¹). Other characteristic bands for the C=O···H- -Cl complex are the decrease of the ν(C=O) mode (-46 cm⁻¹), the increase of the out-of-plane γ(C=O) mode (+14 cm⁻¹), and the frequency decrease of the ν(NH) mode by 14 cm⁻¹. In the case of the N···H- -Cl complex,

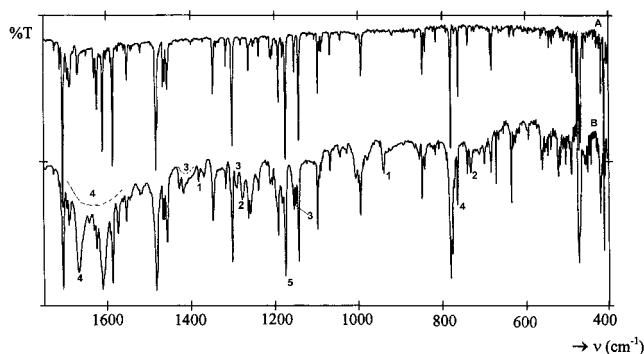


Figure 1. Matrix FT-IR spectrum (1800–400 cm^{-1}) of 2-hydroxypyridine \leftrightarrow 2-oxypyridine/Ar (A) and 2-hydroxypyridine \leftrightarrow 2-oxypyridine/HCl/Ar (HCl:Ar = 1:100) (B) [1, complex $\text{N}^+\text{H}\cdots\text{Cl}^-\cdots\text{H}-\text{O}$; 2, $\text{C}=\text{O}^+\text{H}\cdots\text{Cl}^-\cdots\text{H}-\text{N}$; 3, $\text{N}\cdots\text{H}-\text{Cl}$; 4, $\text{C}=\text{O}\cdots\text{H}-\text{Cl}$; 5, $\text{H}\cdots\text{H}-\text{Cl}$].

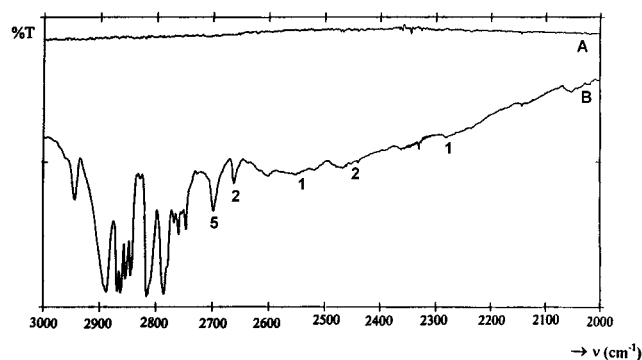


Figure 2. Matrix FT-IR spectrum (3000–2000 cm^{-1}) of 2-hydroxypyridine \leftrightarrow 2-oxypyridine/Ar (A) and 2-hydroxypyridine \leftrightarrow 2-oxypyridine/HCl/Ar (HCl:Ar = 100) (B) [1, 2, 3, 4, 5, see Figure 1].

characteristic bands are found at 1289 and 1181 cm^{-1} , which can be assigned to the shifted $\nu(\text{CO})$ (-10 cm^{-1}) and $\delta(\text{OH})$ ($+8 \text{ cm}^{-1}$) modes, respectively. In Figure 1 two further new bands observed at 936 and 730 cm^{-1} can be interpreted as the out-of-plane modes of the NH^+ and OH^+ groups in the proton-transfer or type III complexes, $\text{N}^+\text{H}\cdots\text{Cl}^-\cdots\text{H}-\text{O}$ and $\text{C}=\text{O}^+\text{H}\cdots\text{Cl}^-\cdots\text{H}-\text{N}$, respectively. The corresponding in-plane bending modes $\delta(\text{NH}^+)$ and $\delta(\text{OH}^+)$ are observed at 1367 and 1276 cm^{-1} . The high-frequency spectral region (3000–2000 cm^{-1}) is illustrated in Figure 2. The stretching modes $\nu(\text{NH}^+)$ and $\nu(\text{OH}^+)$ appear as rather broad bands situated at 2600–2500 and 2500–2400 cm^{-1} . These frequency values are similar to those observed for trimethylaminoxide/HCl⁴⁴ ($\nu(\text{NH}^+) = 2500 \text{ cm}^{-1}$) and uracil/HCl¹³ ($\nu(\text{OH}^+) = 2520\text{--}2455 \text{ cm}^{-1}$). Further evidences for closed H-bonded complexes are the bands observed at 2662 and 2270 cm^{-1} corresponding to $\nu(\text{NH})$ and $\nu(\text{OH})$, respectively. The $\text{H}-\text{O}\cdots\text{H}-\text{Cl}$ complex is manifested in this region by a downward (-171 cm^{-1}) shifted $\nu(\text{HCl})$ located at 2699 cm^{-1} due to the elongation of the $\text{H}-\text{Cl}$ bond. This value is close to the frequency obtained for the $\text{H}_2\text{O}\cdots\text{H}-\text{Cl}$ complex (2699 cm^{-1}).² The relatively small value of this shift implies a type I complex. Other manifestations for the $\text{H}-\text{O}\cdots\text{H}-\text{Cl}$ complex are the decrease of $\nu(\text{OH})$ (-16 cm^{-1}) (Figure 3) and the increase of $\delta(\text{OH})$ ($+11 \text{ cm}^{-1}$).

3.3. Comparison with Calculated Vibrational Data. For each of the five complex systems, only the most characteristic modes have been analyzed by theory. The calculations obtained with B3-LYP and RHF methods in comparison with the experimental matrix results are reported in Table 3. For the $\text{N}^+\text{H}\cdots\text{Cl}^-\cdots\text{H}-\text{O}$ and $\text{C}=\text{O}^+\text{H}\cdots\text{Cl}^-\cdots\text{H}-\text{N}$ complexes, the B3-LYP method predicts much better the ν_{NH^+} and ν_{OH^+}

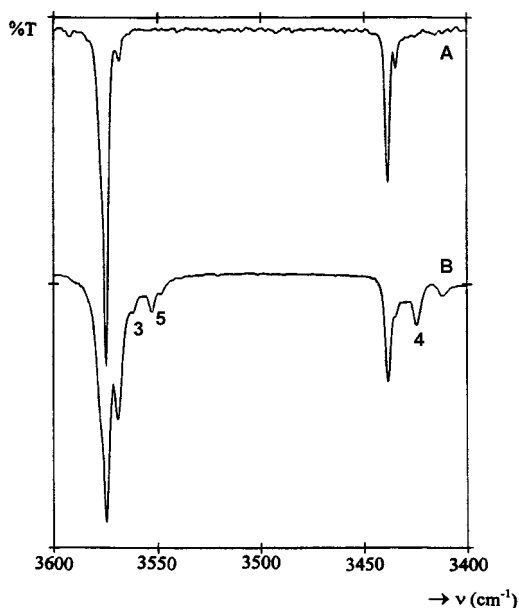


Figure 3. Matrix FT-IR spectrum (3600–3400 cm^{-1}) of 2-hydroxypyridine \leftrightarrow 2-oxypyridine/Ar (A) and 2-hydroxypyridine \leftrightarrow 2-oxypyridine/HCl/Ar (HCl:Ar = 100) (B) [1, 2, 3, 4, 5, see Figure 1].

frequencies in comparison with the RHF method. The shifts $\Delta\nu_{\text{OH}}$ and $\Delta\nu_{\text{NH}}$ are larger, and the agreement between DFT and the experimental values is excellent. On the other hand, both the RHF and DFT methods fail to predict reliable frequencies for δ_{XH^+} and γ_{XH^+} ($\text{X} = \text{N}, \text{O}$). These values, which are presented in the table, are not scaled, because these modes possess a large anharmonicity. For the $\text{N}\cdots\text{H}-\text{Cl}$ and $\text{C}=\text{O}\cdots\text{H}-\text{Cl}$ complexes, the ν_{HCl} modes are observed at 1400 and 1620 cm^{-1} , respectively, and these frequencies suggest an intermediate type I \rightarrow II of hydrogen-bonding. The mechanical anharmonicity of the HCl stretching mode in such complexes may be expected to be large. Therefore, this parameter has been calculated by the variational method.^{39,40} For each complex, the anharmonic frequencies are considerably better predicted with DFT/B3-LYP than with the RHF method, although the computed values are still large compared to the experimental results. This difference can be attributed to a well-known matrix effect. Due to the reduced distances in a solid matrix, a H-bonded complex may be significantly stronger than in the gas phase, and examples of this “matrix fortification” are numerous. The HF stretching frequency in the $\text{NH}_3\cdots\text{HF}$ complex was found to shift from 3215 cm^{-1} in the gas phase to 3041 cm^{-1} in an argon matrix and to 2775 cm^{-1} in a nitrogen matrix.⁴⁵ For the $\text{C}=\text{O}$ stretching modes, B3-LYP gives slightly better results than the RHF method, at least when appropriate scaling factors are used. However, the RHF and DFT methods predict the same δ_{XH} ($\text{X} = \text{N}, \text{O}$) bending frequencies. The HCl stretching mode is situated at 2699 cm^{-1} for the $\text{H}-\text{O}\cdots\text{H}-\text{Cl}$ complex, which suggests a type I hydrogen-bonding. The anharmonic frequencies calculated with B3-LYP and RHF are 2629 and 2977 cm^{-1} , respectively. DFT predicts better the ν_{OH} stretching frequency in comparison with the value obtained by the RHF method. However, both the RHF and DFT/B3-LYP levels of theory agree well with the experimental result for the δ_{OH} bending mode.

4. Conclusions

Computational chemistry combined with matrix-isolation FT-IR spectrometry has been applied to investigate the different H-bonding interactions of 2-hydroxypyridine/2-oxypyridine with

TABLE 3: Vibrational Analysis of 2-Hydroxypyridine and 2-Oxypyridine Complexed with HCl

experiment in Ar ν (cm ⁻¹)	B3-LYP ^b		RHF ^c		assignment
	ν (cm ⁻¹)	I (km·mol ⁻¹)	ν (cm ⁻¹)	I (km·mol ⁻¹)	
					N ⁺ -H...Cl...H-O
2600-2500	2749	3615	3204	807	ν_{NH^+}
2270 (-1304) ^a	2456 (-1313)	695	3444 (-705)	2442	ν_{OH}
1367	1710	544	1865	637	δ_{NH^+}
936	1015	36	1058	57	γ_{NH^+}
					C=O ⁺ -H...Cl...H-N
2662 (-776)	2747 (-858)	3584	3204 (-659)	809	ν_{NH}
2500-2400	2449	728	3444	2442	ν_{OH^+}
1276	1522	66	1642	88	δ_{OH^+}
730	917	34	884	50	γ_{OH^+}
					N...H- -Cl
	3832	87	4194	123	
3562 (-7)	3640 (+1)		3775 (-2)		ν_{OH}
	2162	2769	2901	997	
1400 (-1470)	1831 (-1017)		2729 (-367)		ν_{HCl}^d
	1317	98	1341	26	
1289 (-10)	1284 (-13)		1207 (-5)		ν_{CO}
	1193	68	1293	56	
1181 (+8)	1163 (-5)		1164 (-5)		δ_{OH}
					C=O...H- -Cl
	3599	76	3859	101	
3424 (-14)	3419 (-6)		3473 (-4)		ν_{NH}
	2272	2020	2931	907	
1620 (-1250)	1957 (-891)		2767 (-329)		ν_{HCl}^d
	1706	932	1888	1202	
1666 (-46)	1663 (-47)		1699 (-29)		ν_{CO}
	1453	61	1578	33	
	1417 (-2)		1420 (+1)		δ_{NH}
	772	87	857	116	
775 (+14)	757 (+4)		771 (+3)		γ_{CO}
					H-O...H-Cl
	3763	95	4134	152	
3553 (-16)	3575 (-6)		3721 (-15)		ν_{OH}
	2770	677	3089	367	
2699 (-171)	2629 (-219)		2977 (-119)		ν_{HCl}^d
	1208	154	1305	98	
1177 (+11)	1178 (+10)		1175 (+7)		δ_{OH}

^a Numbers in parentheses correspond to the frequency shift. ^b First row, unscaled values; second row, scaling factor of 0.950 for $\nu(\text{XH})$, 0.980 for γ , and 0.975 for other vibrational modes. ^c First row, unscaled values; second row, uniform scaling factor of 0.900. ^d Anharmonic frequencies.

HCl. On the basis of the interpretation of the IR spectra of the complexes assisted by theoretically calculated energies, frequencies, and intensities, the following three types of hydrogen-bonding have been identified: two closed complexes of type III (ion pair H-bonds), which are the most stable complexes with similar binding energies for the two complexes; two open complexes of intermediate type I \rightarrow II (or nearly symmetrical H-bonds), which also have similar but smaller interaction energies; a weaker complex H-O...H-Cl of type I (weak neutral H-bond).

The DFT predicted frequency shifts $\Delta\nu_{\text{XH}}$ and $\Delta\nu_{\text{XH}^+}$ for the vibrational modes directly involved in the H-bond interactions are much better than those obtained with the RHF method. For the other vibrational modes the two theoretical methods yield predictions with similar accuracy.

The results obtained in this work allow different interactions between nucleic acids and HCl to be interpreted. They also allow further elaborate correlations between particular experimental and calculated parameters such as frequency shifts, H-bond interaction energies, proton affinities, etc.⁴⁶ The use of anharmonic calculated shifts $\Delta\nu_{\text{H-Cl}}$ is recommended to account for the large anharmonicities in these systems. These correlations will be utilized in future interpretations of FT-IR spectra of polyfunctional molecules or complexes modeling nucleic acid bases with HCl.

Acknowledgment. A.D. acknowledges the KU Leuven Research Council for a Research Fellowship. R.R. acknowledges the Belgian IWT for a Research Imbursement.

References and Notes

- (1) Perchard, J. P. In *Matrix-Isolation Spectroscopy*; Barnes, A. J., Orville-Thomas, W. J., Müller; Gauffrès, R., Eds.; NATO Advanced Study Institute; Reidel: Dordrecht, The Netherlands, 1981; pp 551-563.
- (2) Barnes, A. J. *J. Mol. Struct.* **1983**, *100*, 259.
- (3) Barnes, A. J. Personal communication.
- (4) Andrews, L. In *Chemistry and Physics of Matrix-Isolated Species*; Andrews, L., Moskovits, M., Eds.; North-Holland: Amsterdam, 1989; pp 15-46.
- (5) Maes, G. In *Intermolecular Forces. An Introduction to Modern Methods and Results*; Huyskens, P. L., Luck, W. A. P., Zeegers-Huyskens, Th., Eds.; Springer: Berlin, 1991; pp 195-216.
- (6) Lias, S. G.; Liebman, J. F.; Levin, R. D. *J. Phys. Chem. Ref. Data* **1984**, *13*, 695.
- (7) Ault, B. S.; Pimentel, G. C. *J. Phys. Chem.* **1975**, *79*, 615.
- (8) Jeffrey, G. A. *An Introduction to Hydrogen Bonding*; Oxford University Press Inc.: Oxford, 1997; pp 33-55.
- (9) Zundel, G. *Proton Polarizability of Hydrogen-Bonds and Proton Transfer Processes, their Role in Electrochemistry and Biology (Lecture Series)*; Salzberg, 1997.
- (10) Kubelkova, L.; Kotrla, J.; Florian, J. *J. Phys. Chem.* **1995**, *99*, 10285.
- (11) Florian, J.; Kubelkova, L.; Kotrla, J. *J. Mol. Struct.* **1995**, *349*, 435.
- (12) Smets, J.; Graindourze, M.; Zeegers-Huyskens, Th.; Maes, G. *J. Mol. Struct.* **1994**, *318*, 55.

- (13) Graindourze, M.; Smets, J.; Zeegers-Huyskens, Th.; Maes, G. *J. Mol. Struct.* **1994**, *318*, 55.
- (14) Houben, L.; Schoone, K.; Maes, G. *Vibrational Spectrosc.* **1996**, *10*, 147.
- (15) Destexhe, A.; Smets, J.; Adamowicz, L.; Maes, G. *J. Phys. Chem.* **1994**, *98*, 1506.
- (16) Smets, J.; Adamowicz, L.; Maes, G. *J. Mol. Struct.* **1994**, *322*, 113.
- (17) Smets, J.; Adamowicz, L.; Maes, G. *J. Phys. Chem.* **1995**, *99*, 6387.
- (18) Buyl, F.; Smets, J.; Maes, G.; Adamowicz, L. *J. Phys. Chem.* **1995**, *99*, 14697.
- (19) Smets, J.; Adamowicz, L.; Maes, G. *J. Phys. Chem.* **1996**, *100*, 6434.
- (20) Smets, J.; Destexhe, A.; Adamowicz, L.; Maes, G. *J. Phys. Chem.* **1997**, *101*, 6583.
- (21) Van Bael, M. K.; Schoone, K.; Houben, L.; Smets, J.; McCarthy, W.; Adamowicz, L.; Nowak, M. J.; Maes, G. *J. Phys. Chem.* **1997**, *101*, 2397.
- (22) Smets, J.; Destexhe, A.; Adamowicz, L.; Maes, G. *J. Phys. Chem.* **1998**, *102*, 8157.
- (23) Schoone, K.; Smets, J.; Houben, L.; Van Bael, M. K.; Adamowicz, L.; Maes, G. *J. Phys. Chem.* **1998**, *102*, 4863.
- (24) Nowak, M. J.; Lapinski, L.; Fulara, J.; Les, A.; Adamowicz, L. *J. Phys. Chem.* **1992**, *96*, 1562.
- (25) Smets, J.; Maes, G. *Chem. Phys. Lett.* **1991**, *187*, 532.
- (26) Dkhissi, A.; Houben, L.; Smets, J.; Adamowicz, L.; Maes, G. *J. Mol. Struct.* **1999**, *484*, 215.
- (27) Katritzky, A. R.; Szafran, M.; Stevens, J. *J. Mol. Struct.: THEOCHEM* **1989**, *184*, 179.
- (28) Maes, G. *Bull. Soc. Chim. Belg.* **1981**, *90*, 1093.
- (29) Graindourze, M.; Smets, J.; Zeegers-Huyskens, Th.; Maes, G. *J. Mol. Struct.* **1990**, *222*, 345.
- (30) Dkhissi, A.; Adamowicz, L.; Maes, G. *J. Phys. Chem.*, submitted for publication.
- (31) Becke, A. D. *J. Chem. Phys.* **1993**, *98*, 5648.
- (32) Lee, C.; Yang, W.; Parr, R. G. *Phys. Rev.* **1988**, *B37*, 785.
- (33) Chalasin, G.; Szczesniak, M. *Chem. Rev.* **1994**, *94*, 1723.
- (34) Gaussian94, Revision C.3: Frisch, M. J.; Trucks, G. W.; Schlegel, H. B.; Gill, P. M. W.; Johnson, B. G.; Robb, M. A.; Cheeseman, J. R.; Keith, T.; Petersson, G. A.; Montgomery, J. A.; Raghavachari, K.; Al-Laham, M. A.; Zakrzewski, V. G.; Ortiz, J. V.; Foresman, J. B.; Peng, C. Y.; Ayala, P. Y.; Chen, W.; Wong, M. W.; Andres, J. L.; Replogle, E. S.; Gomperts, R.; Martin, R. L.; Fox, D. J.; Binkley, J. S.; Defrees, D. J.; Baker, J.; Stewart, J. P.; Head-Gordon, M.; Gonzales, C.; Pople, J. A., Gaussian Inc., Pittsburgh, PA, 1995.
- (35) Florian, J.; Johnson, B. G. *J. Phys. Chem.* **1994**, *98*, 3681.
- (36) Rauhut, G.; Paulay, P. *J. Phys. Chem.* **1995**, *99*, 3093.
- (37) Florian, J.; Leszczynski, J. *J. Phys. Chem.* **1996**, *100*, 5578.
- (38) Smets, J.; Schoone, K.; Ramaekers, R.; Adamowicz, L.; Maes, G. *J. Mol. Struct.* **1998**, *442*, 201.
- (39) Mijoule, C.; Allavena, G.; Leclercq, J. M.; Bouteiller, Y. *Chem. Phys.* **1986**, *109*, 207.
- (40) Bouteiller, Y.; Latajka, Z.; Ratajczak, H.; Scheiner, S. *J. Chem. Phys.* **1991**, *94*, 2956.
- (41) Del Bene, J. E. *J. Phys. Chem.* **1994**, *98*, 5902.
- (42) Dkhissi, A.; Houben, L.; Smets, J.; Adamowicz, L.; Maes, G. *J. Phys. Chem.* Manuscript in preparation.
- (43) O'Malley, P. J. *J. Am. Chem. Soc.* **1998**, *120*, 11732.
- (44) Barnes, A. J.; Kuzniarski, J. N. S.; Mielke, Z. *J. Chem. Soc., Faraday Trans.* **1984**, *80*, 465.
- (45) Johnson, G. L.; Andrews, L. *J. Am. Chem. Soc.* **1982**, *104*, 3043.
- (46) Smets, J.; McCarthy, W.; Maes, G.; Adamowicz, L. *J. Mol. Struct.* **1999**, *476*, 27.